Protein Film Voltammetry Reveals Distinctive Fingerprints of Nitrite and Hydroxylamine Reduction by a Cytochrome *c* Nitrite Reductase*

Hayley C. Angove‡, Jeffrey. A. Cole§, David J. Richardson‡, and Julea N. Butt‡¶‖

From the ‡Centre for Metalloprotein Spectroscopy and Biology, School of Biological Sciences and ¶School of Chemical Sciences, University of East Anglia, Norwich NR4 7TJ and the §School of Biosciences, University of Birmingham, Birmingham B15 2TT, United Kingdom

The cytochrome *c* nitrite reductases perform a key step in the biological nitrogen cycle by catalyzing the six-electron reduction of nitrite to ammonium. Graphite electrodes painted with *Escherichia coli* cytochrome *c* nitrite reductase and placed in solutions containing nitrite (pH 7) exhibit large catalytic reduction currents during cyclic voltammetry at potentials below 0 V. These catalytic currents were not observed in the absence of cytochrome *c* nitrite reductase and were shown to originate from an enzyme film engaged in direct electron exchange with the electrode. The catalytic current-potential profiles observed on progression from substrate-limited to enzyme-limited nitrite reduction revealed a fingerprint of catalytic behavior distinct from that observed during hydroxylamine reduction, the latter being an alternative substrate for the enzyme that is reduced to ammonium in a two electron process. Cytochrome *c* nitrite reductase clearly interacts differently with these two substrates. However, similar features underlie the development of the voltammetric response with increasing nitrite or hydroxylamine concentration. These features are consistent with coordinated two-electron reduction of the active site and suggest that the mechanisms for reduction of both substrates are underpinned by common rate-defining processes.

An important class of nitrite reductases is composed of the penta-heme containing cytochrome *c* nitrite reductases. One sub-group of cytochrome *c* nitrite reductases is represented by *Escherichia coli* cytochrome *c* nitrite reductase. This enzyme draws electrons from the quinol pool via the *nrfDCB* gene products predicted to be a membrane-bound quinol dehydrogenase, an iron-sulfur protein, and a penta-heme *c*-type cytochrome, respectively (1, 2). The enzymes from *Wolinella succinogenes* and *Sulfurospirillum deleyianum* that draw electrons from the quinol pool via a tetra-heme quinol dehydrogenase, NrfH, typify a second sub-group of cytochrome *c* nitrite reductases (3–5). Both the NrfDCB- and NrfH-dependent nitrite reductases catalyze the six-electron reduction of nitrite to ammonium.

$$NO_2^- + 6e^- + 8H^+ \rightarrow NH_4^+ + 2H_2O$$

REACTION 1

These enzymes also catalyze ammonium production through the five-electron reduction of nitric oxide and the two-electron reduction of hydroxylamine in processes that may contribute to cellular detoxification (6, 7).[1]

The crystal structures of cytochrome *c* nitrite reductases from *E. coli*, *W. succinogenes*, and *S. deleyianum* have recently been reported (4, 8–10). The arrangement of active site residues and heme groups is conserved across all three structures (see Fig. 1 below). A novel *c*-type heme, Heme 1, with lysine and water or hydroxide iron coordination forms the site for substrate binding, and a nearby Ca(II) ion bridges two regions of polypeptide containing key residues for catalysis. Four *c*-type hemes, Hemes 2 through 5, with *bis*-histidine iron coordination accompany Heme 1 and presumably participate in delivering electrons to the active site during catalysis. The hemes are packed in motifs common to a number of proteins, and all nearest neighbor Fe–Fe distances lie below 13 Å. The electrostatic surface of the *E. coli* enzyme around Heme 2 differs from those of the *W. succinogenes* and *S. deleyianum* enzymes and may reflect the distinct redox partners of these enzymes (8).

Spectropotentiometric titrations of the cytochrome *c* nitrite reductases from *E. coli*, *Desulfovibrio vulgaris* Hildenborough and *Desulfovibrio desulfuricans* have established that their redox transformations occur across a wide range of potential (2, 8, 11, 12). For *E. coli* cytochrome *c* nitrite reductase the redox transformations have been interpreted within a structural framework by virtue of the information contained within electron paramagnetic resonance (EPR)[2] spectra (Fig. 1) (8). A rhombic signal having resonances at g $\sim$ 2.91, 2.3, and 1.5 titrates with a mid-point potential at pH 7.0 ($E_{m,7}$) of −37 mV. This signal is characteristic of a *bis*-histidine-coordinated heme Fe(III) having a near parallel alignment of its imidazole rings and is most likely to arise from Heme 2. Broad signals at g $\sim$ 10.8 and 3.5 characteristic of a weakly exchange coupled pair of S = 5/2 and S = 1/2 paramagnets titrate with $E_{m,7}$ = −107 mV. The S = 5/2 center is most likely to be the high spin Fe(III) of Heme 1 whereas the S = 1/2 paramagnet may be nearby Heme 3 or a radical species. A signal with $g_z \sim$ 3.17 characteristic of a *bis*-histidine-coordinated heme Fe(III) with near perpendicular imidazole ring planes titrates with $E_{m,7}$ = −323 mV and has been attributed to either or both of Hemes 4 and 5.

[1] Poock, S. R., Leach, E. R., Moir, J. W. B., Cole, J. A., and Richardson, D. J. (2002) *J. Biol. Chem.* **277,** 23664–23669.
[2] The abbreviations used are: EPR, electron paramagnetic resonance; PFV, protein film voltammetry; PGE, pyrolytic graphite edge.
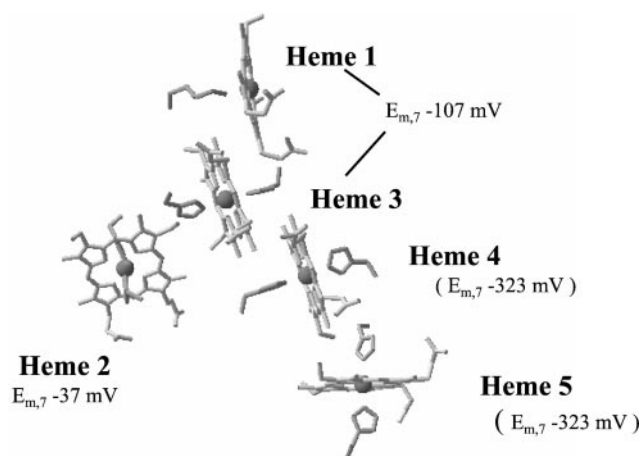
This paper is available on line at http://www.jbc.org

FIG. 1. **The arrangement of heme groups and proteinaceous axial iron ligands in *E. coli* cytochrome *c* nitrite reductase.** The mid-point potentials of the heme centers are as suggested by EPR-monitored spectrophotometric titrations with the caveats discussed in Ref. 8. The Fe–Fe distances are: Hemes 1–3, 9.7 Å; Hemes 2–3, 12.6 Å; Hemes 3–4, 9.4 Å; Hemes 4–5, 11.3 Å. This figure was prepared in Rasmol.

The structure and electrochemical properties of the cytochrome *c* nitrite reductases prompt questions whose answers will underpin an understanding of the mechanism(s) of substrate reduction in these enzymes and about which relatively little is known. For example, can a change of oxidation state at each redox center in the enzyme modulate activity, and if so, is this achieved through changes in electronic or structural properties? Also, given the arrangement of close-packed hemes and in particular the near parallel configuration of Hemes 1, 3, and 4, how are electrons "packaged" for delivery to the substrate and reaction intermediates? Hydroxylamine could be reduced in sequential one-electron steps or a single, concerted two-electron transfer. The possible routes through which the six-electron reduction of nitrite could be achieved are clearly more numerous. There would be an opportunity for the pathways of hydroxylamine and nitrite reduction to overlap if the reduction of nitrite occurs in a series of one- or two-electron transfers (10). However, the initial kinetic study of the *E. coli* enzyme found the Michaelis constant describing hydroxylamine reduction to be more than two orders of magnitude greater than that for nitrite reduction (7). This led to the proposal that hydroxylamine is not a free intermediate in the reduction of nitrite by this enzyme.

Protein film voltammetry (PFV) is a relatively new addition to the range of techniques used to study redox enzymes (13). In this technique the enzyme is immobilized as a (sub-)monolayer, or film, on an electrode surface. Within the film the enzyme undergoes direct electron exchange with the electrode and ideally retains the catalytic properties of the "native" enzyme. When the film contacts a solution of its substrate, the rate at which electrons flow through the enzyme and into the substrate is quantitated by the flow of catalytic current. This current is most informative in the absence of limitations imposed by electron exchange across the electrode:enzyme interface or transport of substrate to the enzyme film. In this situation the current provides a direct measure of the enzyme's intrinsic rate of product formation. This rate will therefore vary in a precise manner in response to defined variation of the electrode potential. For a reductase, variations in activity are defined by changes in the population of reduced, catalytically competent enzyme and the rate-defining step of catalysis. Changes in either of these parameters will give rise to sigmoidal variations of the catalytic current magnitude as the elec-

trochemical potential is varied. As a consequence the catalytic current-potential profiles or waveforms arising from enzyme films frequently show multiple sigmoidal features; *i.e.* features in which the activity may increase *or decrease* as the electrode potential is lowered with a concomitant increase in driving force for the reaction being catalyzed (13–18). It is by visualizing such modulations of activity across the electrochemical potential domain that PFV is able to provide unique insight into the mechanisms of redox enzyme catalysis.

Here we present the first PFV study of a cytochrome *c* nitrite reductase. The catalytic behavior of *E. coli* cytochrome *c* nitrite reductase has been defined on progression from substrate-limited to enzyme-limited catalysis for both nitrite and hydroxylamine reduction. Distinct fingerprints of catalytic behavior are observed in each case; such fingerprints provide important new insight into the mechanisms by which this enzyme directs substrate reduction.

EXPERIMENTAL PROCEDURES

Protein Purification—*E. coli* cytochrome *c* nitrite reductase, NrfA, was purified as described previously and stored as frozen aliquots in liquid nitrogen (8). Activity was measured spectrophotometrically by substrate-dependent oxidation of dithionite-reduced methyl viologen ($\epsilon_{600\ nm} = 13,700\ \text{M}^{-1}\ \text{cm}^{-1}$) in 1 mM methyl viologen, 2 mM CaCl$_2$, 50 mM Hepes, pH 7.0, at 20 °C (8). The samples used in these experiments had a specific activity of 880 μmol of nitrite consumed min^{-1} mg^{-1}, and $A_{410\ nm}/A_{280\ nm}$ = 3.7 for the oxidized enzyme.

Reagent Preparation—Buffer-electrolyte was composed of 2 mM CaCl$_2$, 50 mM Hepes, pH 7.0, unless stated otherwise. Dissolution of the desired mass of NaNO$_2$ in ice-cold buffer-electrolyte gave stock solutions of 25 mM NaNO$_2$. The pH was confirmed as 7.0 after equilibration at 20 °C. Stock solutions of 2 M hydroxylamine were prepared by dissolution of NH$_2$OH·HCl in ice-cold buffer-electrolyte. The pH was adjusted to 7.0 by addition of an appropriate volume of 10 M NaOH, and the solution was brought to the desired volume with buffer-electrolyte. The pH was confirmed as 7.0 upon equilibration at 20 °C. Reagents were of Analar quality or equivalent. Solutions were prepared with water having total nitrogen content < 0.1 ppm (Fisher).
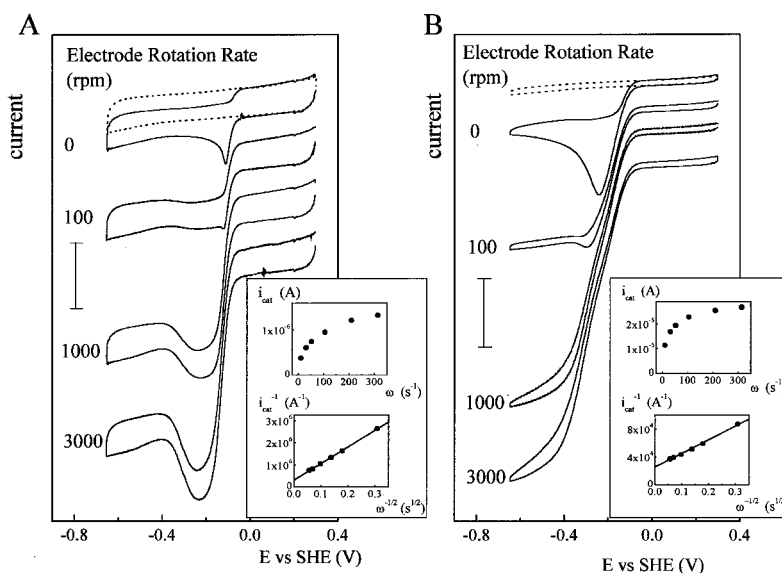
Protein Film Voltammetry—Cyclic voltammetry was performed using a three-electrode cell configuration housed in an N$_2$-filled chamber (atmospheric O$_2$ < 2 ppm) as described previously (14). Pyrolytic graphite edge (PGE) and polycrystalline gold working electrodes of 3-mm diameter were polished immediately prior to use with an aqueous slurry of 0.3-μm Al$_2$O$_3$, sonicated, rinsed, and dried with a tissue. Frozen 5-μl aliquots of 0.6 μM nitrite reductase in 50 mM Hepes, pH 7.0, were taken into the glove box, thawed, and immediately placed on the surface of a freshly prepared working electrode. After approximately 15 s the enzyme solution was removed from the electrode surface, which was then rinsed with room temperature buffer-electrolyte to remove any loosely bound enzyme. Excess buffer-electrolyte was carefully removed from the electrode with a tissue taking care not to dry the electrode surface. The electrode was then placed in the electrochemical cell, and voltammetry commenced. Voltammetry was performed with an Autolab electrochemical analyzer under the control of GPES software. Electrode rotation was with an EG&G model 636 electrode rotator. Potentials are reported with respect to the standard hydrogen electrode by addition of 197 mV to the potential measured with an Ag/AgCl (saturated KCl) reference electrode.

Voltammetric Analysis—The experimentally observed catalytic current magnitude, i_{cat}, was determined at −550 mV as the difference between the measured current and the non-catalytic current, the latter estimated by linear extrapolation of the non-catalytic part of the voltammogram. The rate at which electrons passed through the enzyme film during catalysis was obtained on division of i_{cat} by the Faraday constant (96,484 Coulombs mol electrons^{-1}).

It was found that the catalytic response observed during hydroxylamine reduction was limited only by the properties of the enzyme. In this situation, i_{cat}, can be equated to the flow of current through the enzyme, i_{cat}^{enzyme}, anticipated from a Michaelis-Menten analysis of redox enzyme kinetics,

$$i_{cat}^{enzyme} = \frac{i_{max}C_s}{C_s + K_m} \qquad \text{(Eq. 1)}$$

where i_{max} is the catalytic current observed at the maximum turnover

FIG. 2. **Protein film voltammetry of *E. coli* cytochrome *c* nitrite reductase in 5 and 130 μM nitrite.** *A*, 5 μM nitrite with the electrode rotation rate as indicated, scan rate 10 mV s^{-1}, current marker 0.5 μA. *B*, 130 μM nitrite with the electrode rotation rate as indicated, scan rate 30 mV s^{-1}, current marker 5 μA. In each case a cyclic voltammogram measured in the absence of a nitrite reductase film is shown as a *broken line*. *Inset*, plots of i_{cat} *versus* ω (*upper*) and $(i_{cat})^{-1}$ *versus* $\omega^{-1/2}$ (*lower*) for 5 and 130 μM nitrite. The plotted data were obtained at electrode rotation rates of 100, 300, 500, 1000, 2000, and 3000 rpm for which the corresponding angular velocities (ω) are 10.5, 31.4, 52.4, 105, 209, and 314 s^{-1}. Experiments were performed in 2 mM CaCl$_2$, 50 mM Hepes, pH 7.0, at 20 °C.

rate, C_S the substrate concentration, and K_m the Michaelis constant. Variation of i_{cat} with hydroxylamine concentration was determined in three independent experiments. For each experiment, values of i_{cat} were corrected for the first order loss of signal amplitude with time. K_m was then determined from the variation of the time-corrected catalytic current magnitudes with C_S. Data were fitted to Equation 1 in Microcal Origin using the Levenberg-Marquardt algorithm for non-linear least-squares curve fitting. The value of K_m reported in the text is the average of the three independent experimental determinations. The error reported is that which encompasses the experimentally determined values of K_m.

The catalytic currents observed during nitrite reduction were not limited solely by the properties of the enzyme. The influence of electrode rotation rate on i_{cat} indicated that the catalytic response is limited in part by substrate transport to the enzyme film. To estimate the value of i_{cat}^{enzyme} that would be recorded in the absence of mass transport limitations, *i.e.* at infinitely high electrode rotation rates, the method of Sucheta *et al.* was adopted (18). The value of i_{cat} was related to the electrode rotation rate through the relationship,

$$\frac{1}{i_{cat}} = \frac{1}{i_{cat}^{enzyme}} + \frac{1}{0.62 n \mathrm{FAD}_o^{2/3} \nu^{-1/6} C_s \omega^{1/2}} \qquad (\text{Eq. 2})$$

where ω is the electrode rotation rate expressed as an angular velocity, $\omega = (2\pi \times$ revolutions per minute)/60 s^{-1}. From Equation 2, a plot of i_{cat}^{-1} *versus* $\omega^{-1/2}$ at a given substrate concentration yields $(i_{cat}^{enzyme})^{-1}$ upon extrapolation to $\omega^{-1/2} = 0$. The gradient of this plot is defined by the additional terms in Equation 2, where n is the number of electrons transferred in reduction of the substrate to the product, F is the Faraday constant, A the electrode area, D_o the diffusion coefficient of the substrate, and ν the kinematic viscosity of the solution. For a cytochrome c nitrite reductase film, values of i_{cat} were corrected for loss of magnitude over the time of each experiment, and the subsequent plots of i_{cat}^{-1} against $\omega^{-1/2}$ were linear at each nitrite concentration investigated (Fig. 2, *insets*). Values of i_{cat}^{enzyme} were determined from Equation 2, and K_m was determined from Equation 1 as described above.

RESULTS

Establishing PFV of Cytochrome c Nitrite Reductase—A series of initial experiments established that *E. coli* cytochrome c nitrite reductase is amenable to study by PFV. Freshly polished, pyrolytic graphite edge (PGE) electrodes were covered with solutions containing various concentrations of the enzyme, and the electrodes were then rinsed to remove any loosely bound material and placed in an electrochemical cell

containing a solution of nitrite. Cyclic voltammetry showed that electrodes exposed to a dilute solution (< 2 μM) of the enzyme gave rise to large, negative currents at potentials below approximately 0 V (Fig. 2). These currents indicated that catalytic reduction was occurring at negative potentials. Control experiments provided no evidence for catalytic reduction in the absence of the enzyme (Fig. 2, *dotted lines*). Cytochrome c nitrite reductase is clearly capable of utilizing direct electron exchange with PGE electrodes to drive nitrite reduction. To confirm that the catalytic response originated from an enzyme film, enzyme-coated electrodes were transferred to fresh nitrite-containing solutions where the catalytic response was found to persist with only slight loss of magnitude.

Subsequent studies established that the behavior of cytochrome c nitrite reductase during nitrite reduction was distinct from that during hydroxylamine reduction. The catalytic waveforms describing reduction of each substrate are presented separately below.

Overview of the Behavior Observed during Nitrite Reduction—Cyclic voltammograms arising from films of cytochrome c nitrite reductase in 5 and 130 μM nitrite showed a clear dependence on the rate of electrode rotation (Fig. 2). With the electrode stationary (0 rpm) the sweep toward more negative potentials showed a peak in the reduction current that was absent from the return sweep. This observation was consistent with the presence of a highly active enzyme film that rapidly lowers the concentration of substrate at the electrode surface soon after the onset of catalysis. In agreement with this suggestion, the catalytic current magnitude increased when the electrode was rotated to continually deliver substrate to the enzyme film. Two observations were made as the electrode rotation rate was increased and the rate of substrate delivery to the enzyme film became less of a limitation on the rate of catalysis. First, the catalytic current magnitudes, i_{cat}, increased and approached a constant value (Fig. 2, *insets*). Second, the values of i_{cat} for the forward and reverse sweeps became increasingly superimposable. The form of the catalytic response observed at the highest electrode rotation rates is therefore dominated by the rates of processes intrinsic to the

enzyme and its interaction with substrate.

At the highest electrode rotation rate used in this study (3000 rpm) it was clear that sweeping across the electrochemical potential domain gave rise to distinct modulations of activity in 5 and 130 μM nitrite. At 5 μM nitrite a peak in the rate of substrate reduction was observed at -235 mV on sweeping in *both* directions across the electrochemical potential domain (Fig. 2*A*). The catalytic waveform was unaffected by addition of the reaction product, ammonium. Therefore, product inhibition was not responsible for the decrease in activity observed at lower potentials.

Successive voltammograms recorded from a single enzyme film over a 2-h period showed a slow decrease in magnitude of the catalytic response. The half-life for signal loss was approximately 40 min. Whether the decrease in magnitude was due to film desorption or enzyme inactivation is unclear. Importantly, however, no detectable changes in the shape or position of features in the catalytic waveform were noted over the 2-h period. This is consistent with the response arising from a single form of electrocatalytically active enzyme whose population decreases over the time of the experiment without the formation of new species that contribute to the voltammetric response.

Films of cytochrome *c* nitrite reductase prepared on gold electrodes displayed similar catalytic waveforms to those observed at PGE electrodes. Detailed analysis of the catalytic waveform arising at gold electrodes was precluded by a rapid decrease in signal magnitude during these experiments: the half-life for signal loss was approximately 4 min. However, a clear peak in activity was observed on both the forward and reverse potential sweeps at approximately -253 mV. PGE and gold electrodes present surfaces of quite different properties for interaction with cytochrome *c* nitrite reductase. The observation of similar variations of activity across the electrochemical potential domain at both electrode materials demonstrates that these variations arise from intrinsic properties of the enzyme. The slight difference in peak potentials exhibited at the electrode materials could reflect the influence of the electrode: protein interface on the reduction potential of the heme center(s) responsible for the modulations of activity.

Detailed film voltammetry was performed on PGE electrodes at scan rates from 5 to 100 mV s^{-1} to assess how effectively the catalytic cycle was coupled to electron transfer events. The catalytic waveform at a given scan rate was obtained as the difference between voltammograms recorded in the presence and absence of an enzyme film. The magnitude, shape, and position of features in the catalytic waveform were invariant across this entire range of scan rates. Interfacial electron exchange between the enzyme and electrode is therefore facile. The rates of chemical and intramolecular electron transfer events of catalysis are also sufficiently rapid not to become uncoupled from interfacial electron transfer across this range of scan rates. Indeed it is known that this enzyme exhibits a turnover number of 770 s^{-1} during nitrite-dependent oxidation of dithionite-reduced methyl viologen, which corresponds to passage of 4620 electrons s^{-1} (8). For comparison, *Paracoccus pantotrophus* nitrate reductase, NarGH, which exhibits a turnover number of approximately 30 s^{-1} in assays of nitrate-dependent oxidation of dithionite-reduced methyl viologen corresponding to a flux of 60 electrons s^{-1}, displayed catalytic waveforms that are attenuated at scan rates greater than 40 mV s^{-1} (15).

The catalytic waveform recorded in 130 μM nitrite under conditions of least limitation from substrate mass transport was clearly distinct from that recorded in 5 μM nitrite (Fig. 2). At both PGE and gold electrodes two reversible, sigmoidal
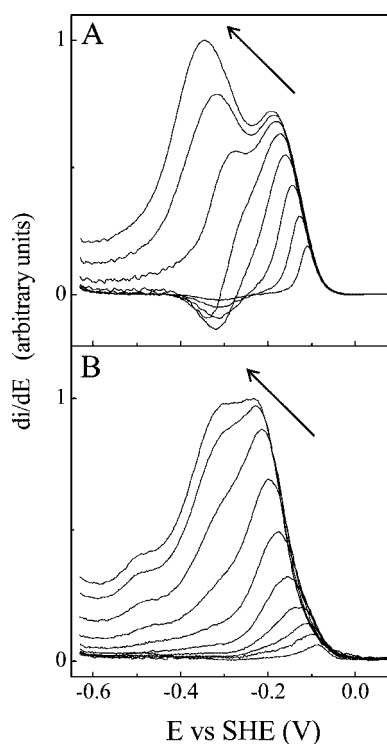

FIG. 3. **First derivatives of the catalytic current with respect to applied potential for films of cytochrome *c* nitrite reductase-catalyzing nitrite and hydroxylamine reduction.** *A*, catalytic current derivatives for nitrite concentrations of 1.7, 3.4, 7, 14, 28, 63, 130, and 265 μM. *B*, catalytic current derivatives for hydroxylamine concentrations of 1.1, 2.2, 4.4, 8.9, 17, 34, 52, 139, 246, and 374 mM. The *arrow* indicates the direction of increasing substrate concentration in each case. The data in each panel were collected from a single enzyme film on titration of substrate into the electrochemical cell and are presented with no correction for the observed loss of signal amplitude with time (see text for details). Experimental conditions are as given in Fig. 2.

increases of activity centered on approximately -184 and -312 mV accompanied the lowering of the electrode potential. These features are more clearly resolved in a plot of the first derivative of the catalytic current with respect to applied potential described below (Fig. 3*A*).

There were negligible differences between the catalytic waveforms recorded at scan rates from 20 to 200 mV s^{-1}. However, unexpected behavior was observed at scan rates below 20 mV s^{-1}. Here, as the potential was swept to more negative values, the activity became progressively smaller than that recorded at the higher scan rates. On returning to more positive potentials the activity of the film continued to decrease relative to that obtained on the forward sweep. At these slower scan rates prolonged exposure of the film to more negative potentials was causing inactivation of the enzyme film and an inequality in the catalytic current magnitudes measured at a given potential on the forward and reverse sweeps. The inequality became more pronounced when CaCl$_2$ was omitted from the experiments. Optimum equality of the forward and reverse catalytic currents required the presence of >0.5 mM CaCl$_2$, and experiments were routinely performed in the presence of 2 mM CaCl$_2$. Interestingly there was no detectable influence of MgCl$_2$ on the catalytic voltammetry. In the presence of 2 mM MgCl$_2$ the catalytic voltammetry was indistinguishable from that observed in the absence of CaCl$_2$.

A possible origin for the specific role of Ca(II) ions in determining the voltammetry of cytochrome *c* nitrite reductase lies in the presence of a structurally conserved Ca(II) ion associated with the enzyme's active site (4, 8, 10). The importance of this

Ca(II) ion in the catalytic process was illustrated in studies of the *S. deleyianum* enzyme where Ca(II) ion dissociation resulted in a decrease in activity that was reversed on re-association of Ca(II) (6). The slow inactivation of films of *E. coli* cytochrome *c* nitrite reductase may then reflect an absence of the active site Ca(II) ion, perhaps resulting in a failure of the enzyme to efficiently process reaction intermediates and leading to a subsequent deviation from the "normal" catalytic cycle. However, the structure of the *E. coli* enzyme reveals a second Ca(II) ion, coordinated between Hemes 3 and 4, and it cannot be excluded that dissociation of this Ca(II) ion contributes to the voltammetric behavior (8). Further experiments established that the activity lost on poising the enzyme film at -450 mV for 60 s was recovered after poising the film at 100 mV for 30 s. Thus, although it was not possible to conclusively identify the cause of the decrease in activity triggered by exposure to low potentials (although see below), the effect is clearly reversed by exposure to more positive electrode potentials and presumably oxidation of centers within the enzyme.

Estimation of the Kinetic Parameters Describing Nitrite Reduction by the Enzyme Film—As described fully under "Experimental Procedures," the method of Sucheta *et al.* was employed to estimate the activity of the enzyme film in the absence of limitations from substrate delivery to the film, i_{cat}^{enzyme}, *i.e.* at infinitely high electrode rotation rates (18). A scan rate of 30 mV s^{-1} was employed to ensure the catalytic current magnitudes of the forward and reverse potential sweeps were close to unity across the range of nitrite concentrations investigated. A typical plot illustrating the variation of i_{cat}^{enzyme} with nitrite concentration for a single film of cytochrome *c* nitrite reductase is shown in Fig. 4*A*.

The value of K_m, 25 ± 2 μM (average of three determinations), is in excellent agreement with the value of 28 ± 3 μM determined in spectrophotometric assays of the enzyme under comparable conditions (8). These results indicate that the enzyme has undergone minimal, if any, perturbation upon incorporation into the electrode-immobilized film.

To define the turnover number of the electrode-immobilized enzyme, the population of electrocatalytically active enzyme must be known. In favorable cases this can be determined by integration of the voltammetric response observed in the absence of substrate, and which will be comprised of a series of wave pairs corresponding to reduction and oxidation of centers in the enzyme (13, 17, 18). Unfortunately, it has not yet been possible to detect such signals from cytochrome *c* nitrite reductase, even when enzyme films that give rise to clear catalytic currents in the presence of nitrite were transferred into solutions lacking substrate or containing inhibitors. Rather, the voltammograms were indistinguishable from those obtained in the absence of enzyme (Fig. 2, *broken lines*). From the dimensions of the cytochrome *c* nitrite reductase monomer, which approximates to a sphere of radius 30 Å, an enzyme monolayer is predicted to contain $\sim 5 \times 10^{-12}$ mol cm^{-2}. Voltammetry of an electrode covered to greater than 25% of a monolayer should give rise to clearly visible signals due to reduction and oxidation of the enzyme's redox centers (15). The surface population of electroactive cytochrome *c* nitrite reductase in these experiments should be significantly less than a monolayer. If it is assumed that the population of electroactive enzyme comprises 25% of a monolayer, then from the typical current densities observed during nitrite reduction at the enzyme-limited maximal rate (approximately 0.3 mA cm^{-2} at -550 mV) a lower limit for the turnover number of molecules in the film is calculated to be 370 s^{-1}. Molecules of cytochrome *c* nitrite reductase within the film therefore support a flux of at least 2230 electrons s^{-1} at the maximum turnover rate. This compares favor-
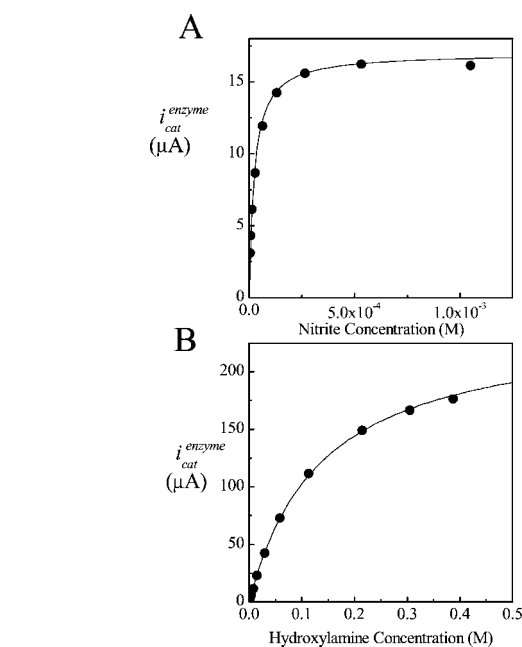

FIG. 4. **Representative variations of the catalytic current magnitude with substrate concentration for films of *E. coli* cytochrome *c* nitrite reductase.** *A*, nitrite concentrations 3.4, 7, 14, 28, 63, 130, 265, 532, and 1050 μM. The *solid line* describes the catalytic current arising from a Michaelis-Menten description of enzyme kinetics with $K_m = 24$ μM and $i_{max} = 17$ μA. *B*, hydroxylamine concentrations were 0.6, 1.25, 1.9, 3.7, 7.5, 15, 30, 58, 113, 214, 305, and 387 mM. The *solid line* describes the catalytic current arising from a Michaelis-Menten description of enzyme kinetics with $K_m = 137$ mM and $i_{max} = 243$ μA. Experimental conditions are as given in Fig. 2.

ably with the flux of 4620 electrons s^{-1} measured in spectrophotometric assays (8).

Development of the Catalytic Waveform on Progression from Nitrite-limited to Enzyme-limited Catalysis—The high activity of the nitrite reductase film has prevented voltammetry from being recorded under conditions where the influence of electrode rotation rate and hence limitation by substrate delivery is completely absent. However, the voltammograms recorded at the higher rotation rates clearly converged toward a limiting response for which the predominant influences are the intrinsic properties of the enzyme-substrate interaction (Fig. 2). Under these conditions and utilizing a scan rate of 30 mV s^{-1}, the catalytic wave is found to be independent of the direction of the potential sweep, and all modulations of activity observed on traversing the electrochemical potential domain are fully reversible.

At the lowest nitrite concentrations for which a clear catalytic waveform could be resolved, two sigmoidal features were clearly present. On sweeping toward more negative potentials in 1.7 μM nitrite, an increase in activity was centered on -105 mV and had a steepness close to that anticipated for a concerted two-electron process (Fig. 5*A*). The activity then showed an approximately constant and maximal value before it decreased to approach a potential-independent value in a feature centered on -320 mV with the steepness of a one-electron process. Sequential increase of the nitrite concentration resulted in a broadening of the higher potential sigmoidal feature and its displacement toward more negative potentials (Fig. 2*A*). At the same time, the decrease in activity observed on sweeping toward more negative potentials became less distinct. At nitrite concentrations above approximately 60 μM a second sigmoidal increase of activity became increasingly pronounced over the lower potential region of the voltammetric sweep (Fig. 2*B*).

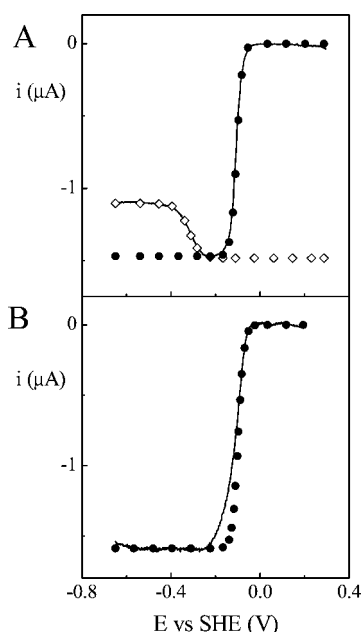Plots of the first derivative of the catalytic current with

FIG. 5. **Baseline-subtracted protein film voltammetry from cytochrome *c* nitrite reductase in 1. 7 *μ*M nitrite and 1.2 mM hydroxylamine.** *A*, *solid line*, the response in 1.7 *μ*M nitrite; *circles*, a Nernstian plot having $n = 2$ and $E_m = -105$ mV; *diamonds*, a Nernstian plot having $n = 1$ and $E_m = -320$ mV. *B*, *solid line*, the response in 1.2 mM hydroxylamine; *circles*, a Nernstian plot having $n = 2$ and $E_m = -98$ mV. Voltammograms were recorded at a scan rate of 20 mV s^{-1} with electrode rotation at 3000 rpm, other details are as in Fig. 2.

respect to applied potential provide a convenient way to visualize the development of the catalytic waveform with increasing nitrite concentrations (Fig. 3*A*). At the lowest nitrite concentrations investigated, the catalytic current derivatives show both a positive and a negative feature due to the local maximum in activity observed on sweeping across the electrochemical potential domain. The positive feature occurs at higher potentials and reflects that region of the waveform where the catalytic activity increases reversibly as the electrode potential is lowered. The negative feature occurs at lower potentials where the activity decreases reversibly as the electrode potential is lowered. On raising the nitrite concentration, the positive component of the derivative shifts toward more negative potentials and broadens, and a shoulder appears on its low potential flank. Simultaneously, the negative feature is lost from the derivatives. At highest nitrite concentrations the peaks apparent in the catalytic current derivatives reflect the two reversible, sigmoidal increases in activity, which accompanied lowering of the electrode potential. A characteristic fingerprint of the nitrite reductase activity of cytochrome *c* nitrite reductase was obtained by overlaying the catalytic current derivatives reflecting catalysis at a range of nitrite concentrations (Fig. 3*A*).

Overview of the Behavior Observed during Hydroxylamine Reduction—Hydroxylamine concentrations greater than 500 *μ*M were needed to detect appreciable catalytic currents from films of cytochrome *c* nitrite reductase (Fig. 5*B*). The catalytic response was essentially independent of the electrode rotation rate at each hydroxylamine concentration investigated. The waveforms were therefore free from any significant limitations due to substrate delivery to the enzyme film, and experiments were routinely performed at a single electrode rotation rate of 3000 rpm. The catalytic waveforms of the forward and reverse sweeps were in good agreement for scan rates from 5 to at least 50 mV s^{-1}. The catalytic waveforms were also insensitive to variations of the CaCl$_2$ concentration or the presence of MgCl$_2$.

The insensitivity of the hydroxylamine reductase activity to changes of Ca(II) ion concentration contrasted with the behavior observed during nitrite reduction. The structures of substrate-bound *W. succinogenes* cytochrome *c* nitrite reductase provide a possible explanation for these different behaviors (9). The iron of Heme 1 coordinates the substrate nitrogen atom in both the nitrite- and hydroxylamine-bound enzymes. The oxygen atoms of nitrite coordinate Arg-114 and His-277, the latter being located on a loop of polypeptide positioned by the structurally conserved Ca(II) ion. The hydroxylamine oxygen atom coordinates only Arg-114. As a consequence, hydroxylamine has no direct interaction with that region of the active site positioned by the structurally conserved Ca(II) ion. The observation that Ca(II) ion concentrations influence only the nitrite reductase activity of the *E. coli* enzyme suggests that dissociation of Ca(II) from the active site, rather than from the binding site located between Hemes 3 and 4, gives rise to the observed effects.

Estimation of the Kinetic Parameters for Hydroxylamine Reduction—A typical plot showing the variation of i_{cat}^{enzyme} with hydroxylamine concentration arising from a film of cytochrome *c* nitrite reductase is presented in Fig. 4*B*. Control experiments performed with freshly polished PGE electrodes and hydroxylamine concentrations above 60 mM showed the presence of broad waves corresponding to non-enzymatic reduction and oxidation processes. Inhibition of the cytochrome *c* nitrite reductase film with cyanide showed that the non-enzymatic contribution to the voltammetry was suppressed by the presence of the enzyme film. The non-enzymatic contribution to the total catalytic current was found to be less than 2% of that measured in 400 mM hydroxylamine. Experiments were restricted to hydroxylamine concentrations below this level to ensure minimal impact of the non-enzymatic response on the PFV of cytochrome *c* nitrite reductase. Several independent experiments produced results similar to those of Fig. 5*B* and from which a value of $K_m = 127 \pm 25$ mM was defined.

Transfer of an enzyme film from a solution containing 400 *μ*M nitrite to one containing 40 mM hydroxylamine caused a 3.5-fold increase in catalytic current magnitude. The maximum electron flux during hydroxylamine reduction can be calculated to be at least 14-fold greater than that observed during nitrite reduction. For an enzyme film comprised of 25% of a monolayer, this corresponds to a flux of 31,220 electrons s^{-1} and a turnover number of 15,610 s^{-1}. By contrast spectrophotometric assays of hydroxylamine turnover yielded $K_m = 30 \pm 4$ mM and a turnover number of 2382 s^{-1}, corresponding to a maximum electron transfer rate of 4764 electrons s^{-1}, the latter value being only slightly greater than that measured for nitrite reduction (8). The different enzyme activities reported by the two methods are readily explained if the PFV response is limited by intrinsic properties of cytochrome *c* nitrite reductase whereas the spectrophotometric assays are limited by the assay conditions.

Development of the Catalytic Waveform on Progression from Hydroxylamine-limited to Enzyme-limited Turnover—Catalytic current derivatives summarizing the waveforms observed in hydroxylamine concentrations ranging from ~1 to 375 mM are presented in Fig. 3*B*. The fingerprint of hydroxylamine reductase activity is clearly distinct from that obtained during the reduction of nitrite. The catalytic current derivatives for hydroxylamine limited turnover contain a single positive feature that reflects the increase in activity observed on scanning toward more negative potentials. For a hydroxylamine concentration of 1.2 mM the increase in activity was centered on −98 mV and had the steepness associated with a concerted two-electron process at higher potentials but broadened at lower

potentials (Fig. 5*B*). On increase of the hydroxylamine concentration the catalytic wave broadened and was displaced toward more negative potentials. At the highest hydroxylamine concentrations investigated the waveform displayed two prominent sigmoidal increases in activity centered on approximately −230 and −300 mV, and reflected in the peaks of the corresponding catalytic current derivatives. A small increase in i_{cat} centered on −500 mV was persistently revealed in the catalytic current derivatives obtained at the higher hydroxylamine concentrations (Fig. 3*B*).

DISCUSSION

PFV has clearly established that the catalytic currents measured during substrate reduction by *E. coli* cytochrome *c* nitrite reductase are determined not only by the identity and concentration of the substrate but also the electrochemical potential experienced by the enzyme. The distinct patterns of behavior observed during nitrite and hydroxylamine reduction highlight how the dependence of enzyme activity on applied potential cannot be simply predicted from knowledge of the reduction potentials describing centers within the enzyme. Rather, PFV reveals the exquisite sensitivity of cytochrome *c* nitrite reductase to control from a variety of factors.

PFV is most informative when it reflects the intrinsic properties of an enzyme (13). These properties should be independent of the technique used to study the enzyme, and ideally the enzyme will exhibit these properties in its natural environment. The catalytic waveforms observed during the PFV of cytochrome *c* nitrite reductase do not appear to be significantly limited by rates of electron exchange across the electrode:protein interface. The catalytic currents observed at the higher hydroxylamine concentrations used in this study are much greater than those observed during nitrite reduction. The waveforms are also largely free from limitations due to substrate delivery to the enzyme film at the highest electrode rotation rates of this study. The integrity of enzyme molecules within the film is therefore most readily assessed by comparison of their catalytic behavior with that observed during solution phase assays under equivalent conditions. This is made possible by the nature of the cyclic voltammetric experiment in which the catalytic current provides a direct measure of the rate at which electrons flow through the enzyme film and into substrate. The K_m values exhibited by films of cytochrome *c* nitrite reductase during nitrite and hydroxylamine reduction differ by approximately three orders of magnitude, in agreement with the behavior observed in parallel solution assays (8). A lower estimate of the turnover number describing nitrite reduction by the film is also in agreement with that found in solution assays. However, hydroxylamine reduction by the films occurs with a turnover number at least 6-fold greater than that measured in the solution assay. In this case the voltammetric experiment is clearly free from a limitation imposed by the conditions of the solution assay.

Calculation of absolute turnover numbers for cytochrome *c* nitrite reductase within the film is prevented by uncertainty in the number of molecules that give rise to the catalytic response. Nevertheless, a wealth of information on those factors that determine the activity of the enzyme is provided by the distinct *variations* of activity observed on sweeping across the electrochemical potential domain. These variations of activity are readily interpreted in a film voltammetric experiment, because the oxidation state of each redox center in the enzyme population under study is under the control of the electrode potential at all times. In the absence of substrate, the redox centers will be switched between their accessible oxidation states in a Nernstian fashion as the electrode potential is swept linearly across the electrochemical potential domain. On introducing

substrate into such an experiment at a concentration well below the K_m, a small percentage of the enzyme population will interact with the substrate at any given time and therefore at any given potential. At each potential the rate of catalysis will therefore reflect the population of enzyme molecules primed to pass electrons to the substrate. For a reductase in which the only redox active group is that associated with the active site this population will be that containing a reduced active site. The catalytic current will therefore increase in a sigmoidal fashion on sweeping toward more negative potentials and reflect a Nernstian titration of the active site (15, 17). When the oxidation states of additional redox centers in an enzyme contribute to the definition of its activity, additional sigmoidal features will appear in the voltammetry (13–18). When the reduction potentials of those centers defining changes of activity across the electrochemical potential domain are sufficiently well separated, the features in the voltammogram will reflect a Nernstian titration of each center whose oxidation state exerts regulatory control. The magnitude and direction of each sigmoidal change in activity will be governed by the difference between the rate of product formation when the redox center in question is 100% oxidized and that when it is 100% reduced.

The PFV of cytochrome *c* nitrite reductase during substrate limited reduction of nitrite and hydroxylamine shows that activity is initiated by reduction of a constituent of the active site with a reduction potential in the vicinity of −100 mV. For both substrates the steepness of the corresponding voltammetric feature is consistent with coordinated two-electron reduction of this redox center. Correlating these observations with the EPR spectroscopic and equilibrium electrochemical properties of this enzyme, it is most likely that the centers giving rise to the spin-coupled pair ($E_{m,7}$ = −107 mV) are those that define the redox chemistry of the active site (8). The redox chemistry of Heme 1 is effectively coupled to that of Heme 3 or a nearby amino acid, such as Tyr-216, to provide a site for coordinated exchange of two electrons. An active site loaded with two electrons will provide sufficient reducing equivalents for the two-electron reduction of hydroxylamine to ammonia. To perform the six-electron reduction of nitrite to ammonia, additional electrons must be drawn through the active site. Once the active site is reduced and nitrite is bound, the additional electrons required for ammonia formation will flow rapidly through the enzyme from the electrode driven by the strong driving force for product formation ($E_{m,7}$ NO_2^-/NH_4^+ = + 340 mV). The flow of these additional electrons contributes to the magnitude of the catalytic response at each potential. However, the shape and position of the waveform remain defined by the population of catalytically competent enzyme present at each electrode potential.

The features describing reduction of the active site during nitrite and hydroxylamine reduction show a slight difference in their steepness that may reflect a different stability of the semi-reduced active site during each catalytic process (17). Such behavior could arise if the reduction potentials of the active site are different in each case. For cytochrome *c* nitrite reductase the possibility, that hydroxylamine is an intermediate on the pathway of nitrite reduction and therefore bound to the active site in the oxidized, semi-reduced and reduced forms, provides a possible reason for the active site exhibiting distinct properties during each catalytic process.

PFV of cytochrome *c* nitrite reductase has also visualized how reduction of a one-electron center having a reduction potential of approximately −320 mV leads to a decrease of activity during nitrite-limited reduction. This center is most likely to be provided by Heme 4 and/or 5 ($E_{m,7}$ = −323 mV) (8). Reduction of the low potential heme may modify the activity of

the enzyme through modulation of its electronic properties or a conformational change; the latter has been suggested to occur on reduction of *D. desulfuricans* cytochrome *c* nitrite reductase (12). Whichever mechanism is responsible for the decrease in nitrite reductase activity triggered by exposing the enzyme to "low" potentials, it is of considerable note that such behavior is not observed during hydroxylamine reduction.

For both nitrite and hydroxylamine reduction, clear changes in the catalytic waveform are observed on progression from substrate-limited to enzyme-limited turnover. The voltammetry still reflects the population of reduced, catalytically primed enzyme present at each potential, but this population becomes increasingly defined by the rates of chemical and/or electrochemical events in the catalytic cycle as the substrate concentration is raised (13, 14). The waveforms develop in a similar manner on increase of the hydroxylamine or nitrite concentration. The response becomes displaced toward more negative potentials, broadens, and a second increase in current appears at lower potentials. The observations suggest that similar rate-defining events underlie substrate reduction in both cases. They are consistent with the rate of enzyme-limited catalysis being defined by the rate of electron delivery to the active center and most likely gated by a chemical event (17, 20). The differences between the absolute responses recorded in each substrate will reflect differences in the rate constants and reduction potentials specific to the catalytic cycle describing reduction of each substrate. Interestingly, our inspection, of the solution voltammetry of *D. desulfuricans* cytochrome *c* nitrite reductase under conditions supporting a maximum nitrite reduction rate and measured with a view to development of a nitrite biosensor, shows a catalytic waveform of similar shape to that observed during PFV of the *E. coli* enzyme (19, 21). This suggests that the description of enzyme-limited substrate reduction uncovered by PFV will be common to the cytochrome *c* nitrite reductases, in agreement with the conservation of active site structure and heme packing motifs recently revealed by structural studies of this important family of enzymes.

REFERENCES

1. Hussain, H., Grove, J., Griffiths, L., Busby, S., and Cole, J. (1994) *Mol. Microbiol.* **12,** 153–163
2. Eaves, D. J., Grove, J., Staudenmann, W., James, P., Poole, R. K., White, S. A., Griffiths, I., and Cole, J. A. (1998) *Mol. Microbiol.* **28,** 205–216
3. Simon, J., Gross, R., Einsle, O., Kroneck, P. M. H., Kröger, A., and Klimmek, O. (2000) *Mol. Microbiol.* **35,** 686–696
4. Einsle, O., Stach, P., Messerschmidt, A., Simon. J., Kröger, A., Huber, R., and Kroneck, P. M. H. (2000) *J. Biol. Chem.* **275,** 39608–39616
5. Simon, J., Pisa, S., Stein, T., Eichler, R., Klimmek, O., and Gross, R. (2001) *Eur. J. Biochem.* **268,** 5776–5782
6. Stach, P., Einsle, O., Schumacher, W., Kurun, E., and Kroneck, P. M. H. (2000) *J. Inorg. Biochem.* **79,** 381–385
7. Kajie, S., and Anraku, Y. (1986) *Eur. J. Biochem.* **154,** 457–463
8. Bamford, V. A., Angove, H. C., Seward, H. E., Thomson, A. J., Cole, J. A., Butt, J. N., Hemmings, A. M., and Richardson, D. J. (2002) *Biochemistry* **41,** 2921–2931
9. Einsle, O. (2001) in *Handbook of Metalloproteins*, (Messerschmidt, A., Huber, R., Poulos, T., and Wieghardt, K., eds) Vol. 1, pp. 440–453, John Wiley & Sons, Ltd., New York
10. Einsle, O., Messerschmidt, A., Stach, P., Bourenkov, G. P., Bartunik, H. D., Huber, R., and Kroneck, P. M. H. (1999) *Nature* **400,** 476–480
11. Pereira, I. A. C., LeGall, J., Xavier, A. V., and Teixeira, M. (2000) *Biochim. Biophys. Acta* **1481,** 119–130
12. Costa, C., Moura, J. J. G., Moura, I., Wang, Y., and Huynh, B. H. (1996) *J. Biol. Chem.* **271,** 23191–23196
13. Armstrong, F. A., Heering, H. A., and Hirst, J. (1997) *Chem. Soc. Rev.* **26,** 169–179
14. Anderson, L. J., Richardson, D. J., and Butt, J. N. (2001) *Biochemistry* **40,** 11294–11307
15. Anderson, L. J., Richardson, D. J., and Butt, J. N. (2000) *Faraday Discuss.* **116,** 155–169
16. Butt, J. N., Thornton, J., Richardson, D. J., and Dobbin, P. S. (2000) *Biophys. J.* **78,** 1001–1009
17. Heering, H. A., Hirst, J., and Armstrong, F. A. (1998) *J. Phys. Chem. B* **102,** 6889–6902
18. Sucheta, A., Cammack, R., Weiner, J., and Armstrong, F. A. (1993) *Biochemistry* **32,** 5455–5465
19. Scharf, M., Moreon, C., Costa, C., Van Dijk, C., Payne, W. J., LeGall, J., Moura, I., and Moura, J. J. G. (1995) *Biochem. Biophys. Res. Commun.* **209,** 1018–1025
20. Page, C. C., Moser, C. C., Chen, X. X., and Dutton P. L. (1999) *Nature* **402,** 47–52
21. Moreno, C., Costa, C., Moura, I., Le Gall, J., Liu, M. Y., Payne, W. J., van Dijk, C., and Moura, J. J. G. (1993) *Eur. J. Biochem.* **212,** 79–86